

Kinetic energy distribution for the ionization and dissociation process of C_2H_4 by electron impact

X. Wang^{1,2}, Z. Chen^{1,2}, B. Wei^{1,2}, R. Hutton^{1,2} and Y. Zou^{1,2}

¹Applied Ion Beam Physics Laboratory, Fudan University, Key Laboratory of the Ministry of Education, Shanghai 200433, China

²Institute of Modern Physics, Department of Nuclear Science and Technology, Fudan University, Shanghai 200433, China

E-mail: brwei@fudan.edu.cn

Abstract. The dissociative ionization of ethylene molecules following impact by electrons in the energy range of 20 to 200 eV has been studied with a cold target recoil-ion momentum spectrometer (COLTRIMS). The relative partial cross sections for the ionic fragments $C_2H_n^+$ ($n=0\sim 3$) with respect to $C_2H_4^+$ were plotted as a function of the incident energy. By measuring the time of flight and position of the fragment ions, the kinetic energy distribution has been deduced. Taking advantage of the supersonic jet expansion, the thermal motion contributing to the kinetic energy distribution of the recoil-ions was reduced. The average kinetic energy of the recoil ions as a function of the incident electron energy has also been plotted. Furthermore, the average kinetic energy release for the dissociation to $C_2H_3^+$ and $C_2H_2^+$ were estimated as 0.76 eV and 0.73 eV respectively.

1. Introduction

Atomic and molecular data plays a crucial role in the development of Magnetic Confinement Fusion (MCF), and various types of experimental data on the interaction of Hydrocarbon molecules with electrons are required for understanding of the behavior of these molecules in the edge plasma region [1-3]. Ethylene (C_2H_4) is the simplest unsaturated hydrocarbon with a C=C bond. The cross sections for electron impact ionization of ethylene have been investigated [4-6]. More recently, with time-of-flight (TOF) mass spectrometry and two dimensional ion-ion coincidence techniques, the study of multiply ionized molecules provides a method to identify the contributions for different dissociation pathways [7, 8]. In fact, electron impact ionization and dissociation of hydrocarbon molecules has been widely studied in the past two decades, see, for example, a recent review by D. Reiter and R. T. Janev [9].

During the interaction between electrons and molecules, the ionic and neutral fragments produced often carry away a certain amount of kinetic energy (KE) which is released from the excitation energy left with the parent particle. Investigations of kinetic energy release (KER) are useful to understand such dissociation processes. The previous studies showed that the same fragment ion can be formed in different dissociation processes, while the dissociation process depends on the excitation energy of the parent ions [10-15]. Therefore, fragment ions from different dissociation processes have distinct kinetic energy distributions. Thus to build a model environment for a plasma, we require not only about fragment ion production efficiencies but also their KE distributions [16]. However, the kinetic energy of product ions is sometimes very small, and can even be below the thermal motion energy at



room temperature. This indicates that the thermal motion should be taken into account for precise measurements of the kinetic energy.

In this work, we report the measurement of the kinetic energy distribution of fragmental ions produced through the interaction between an electron beam and a cold hydrocarbon (C_2H_4) target beam. The experiments were carried out by using cold target recoil-ion momentum spectroscopy (COLTRIMS). The incidence beam energies ranged from 20 to 200eV. Taking advantage of supersonic expansion, the thermal contribution of the kinetic energy of the target molecules is much smaller than in previous studies, and, as a result, kinetic energies are recorded more precisely for the dissociative processes. According to the accurate kinetic energy measurement, the mean KER was estimated and used to investigate the different dissociation processes via electron impact.

2. Experiment setup

The present experiment was performed by using COLTRIMS at Fudan University in Shanghai. A schematic diagram of the apparatus used for the present measurements is shown in figure 1. The setup comprises a pulsed electron gun, a three-stage supersonic gas jet, a recoil ion detector with delay-line anode, and a time-of-flight spectrometer. The pulsed electron beam (pulse length ≈ 1 ns, repetition rate 10 kHz), produced by a standard thermal cathode [17], crosses and ionizes a C_2H_4 beam. The cold molecular beam provided by a supersonic gas jet, in which high pressure gas (2 bar) flowed through a 10 μm nozzle into the first stage of the vacuum chamber at room temperature. A 0.1 mm skimmer at a variable distance of about 10 mm downstream of the nozzle was used to extract a geometrically well-defined gas beam. A multistage structure was utilized to keep high vacuum in the collision chamber. The background vacuum in the collision chamber was better than 3×10^{-10} torr during the experiment. A set of Helmholtz coils were used to reduce the earth's magnetic field.

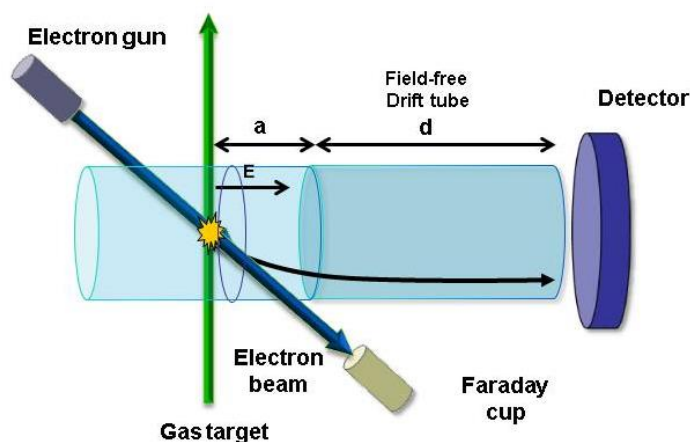


Figure 1. schematic diagram of the apparatus.

The produced recoil ions were accelerated by a pulsed electric field of 25 V/cm and then passed through a field-free drift tube, and finally detected by a 75mm delay-line anode position sensitive detector. The length of the field-free drift tube $d = 2a$ is employed here to reduce the influence of the target size, where a ($=10$ cm) is the length of the extraction field. A VME64x system was used for data acquisition, which contains a Multi-hit Time to Digital Converter (TDC). During the experiment, the recoil ion signals produced the start pulse and the signal from the ultra-fast signal generator was used as a common stop. The coincidence measurements were performed in event by event mode, and the information of the position and timing was recorded. The momentum of the recoil ion can be reconstructed according to the measured position and time information in off-line data analysis.

3. Results and discussion

A typical mass spectrum of the fragments of C_2H_4 impacted by 70 eV electrons is shown in figure 2. The observed ions include the parent ion $C_2H_4^+$ and singly charged fragments such as $C_2H_n^+$ ($n = 0\sim 3$). The peaks of CH_3^+ , CH_2^+ , CH^+ and C^+ are broader because these ions carry higher kinetic energy. We cannot resolve double charged $C_2H_4^{2+}$ from CH_2^+ since they have the same m/q value. The peak marked as '29⁺' in the spectrum originated from of $^{13}CH_2-CH_2^+$, since the natural abundance of ^{13}C is about 1.1%. Both HO^+ and H_2O^+ originated from the background.

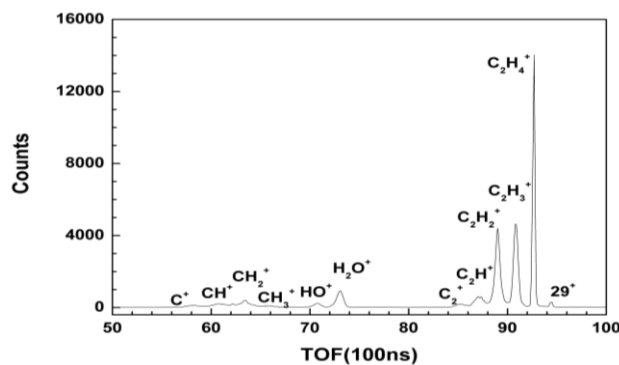


Figure 2. Mass spectrum of C_2H_4 at electron energy of 70 eV.

The cross sections for forming $C_2H_3^+$, $C_2H_2^+$, C_2H^+ and C_2^+ relative to the formation of $C_2H_4^+$ are deduced from the TOF spectra. In figure 3, the relative partial ionization cross sections of $C_2H_n^+$ ($n=0-3$) to $C_2H_4^+$ are plotted as a function of electron energies in the range of 20 to 200 eV. The uncertainty in the present measurement is less than 10% [18], which is mainly due to the counting statistics and overlaps of the peaks.

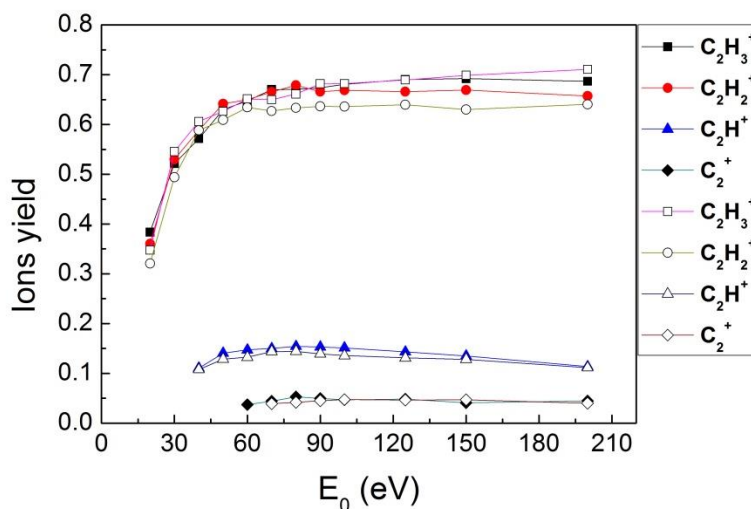


Figure 3. The relative partial ionization cross section for forming $C_2H_3^+$, $C_2H_2^+$, C_2H^+ and C_2^+ following electron ionization of C_2H_4 . The data of the present experiment represented by solid symbol and the open symbol given by Ref. [4]

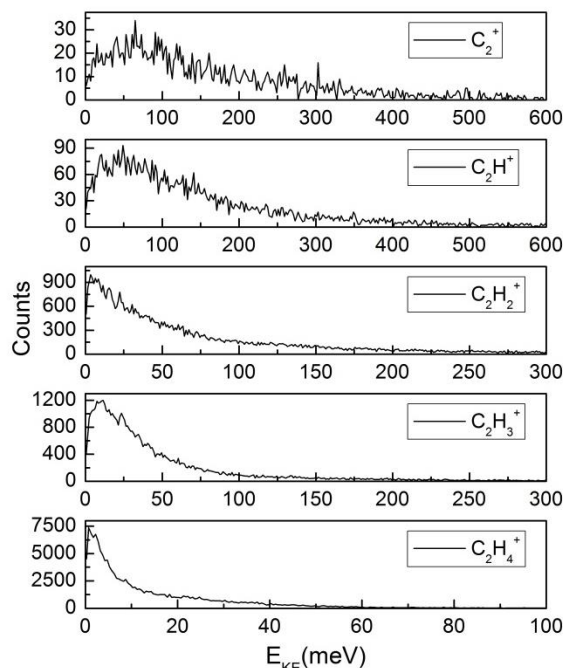


Figure 4. The ion kinetic energy distributions of $C_2H_4^+$, $C_2H_3^+$, $C_2H_2^+$, C_2H^+ and C_2^+ produced in the collision between ethylene molecules and 70 eV electrons. Please note the changed scales for different fragment ion species.

In the present work, we are interested in the kinetic energy release from the dissociation processes related to the ions $C_2H_n^+$ ($n = 0\sim 3$). Figure 4 shows the kinetic energy distribution of the recoil ions produced in the collision between ethylene molecules and 70 eV electrons. The ground state ethylene molecule has the electronic configuration $(1a_g)^2(1b_{1u})^2(2a_g)^2(2b_{1u})^2(1b_{2u})^2(3a_g)^2(1b_{3g})^2(1b_{3u})^2$ [5]. The ionization of an outermost orbital ($1b_{3u}$) electron (binding energy of 10.51 eV) produces a stable ethylene ion in its ground electronic state (X^2B_{3u}). In contrast, the ionization of an electron in a deeper lying orbital can lead to the production of the parent ion $C_2H_4^+$ in an excited state, which is usually unstable and result in a dissociation process. For example, the ejection of a ($1b_{3g}$) electron (binding energy of 13.74 eV) can produce $C_2H_4^+$ ion in its first excited electronic state (A^2B_{3g}) and this has an excitation energy of 3.23 eV. For dissociation of the $C_2H_4^+$ ion via the three channels shown below, the extra energy required above ionization is 2.58 eV 2.72 eV and 7.25 eV for paths (1), (2) and (3) respectively [2].



Ethylene ions in the state (A^2B_{3g}) can dissociate following the pathway (1) and (2). However, the dissociation energy for path (2) is 2.72 eV which is higher than 2.58 eV for path (1). Correspondingly, the KER for path (2) is lower than path (1), and this is shown in figure 4, namely, the distribution of $C_2H_3^+$ has a maximum at about 10 meV while the distribution of $C_2H_2^+$ has a maximum at about 5 meV. To be specific, the ethylene ions can be excited to even higher states and undergoes dissociation for producing ions $C_2H_3^+$ and $C_2H_2^+$ with higher kinetic energies. The reaction channel (3) also can produce $C_2H_2^+$ ions and this gives a contribution to the broader tail of the kinetic energy distribution for $C_2H_2^+$. For the ions C_2H^+ and C_2^+ , the kinetic energy distributions become more broader and Coulomb explosion processes need to be taken into account.

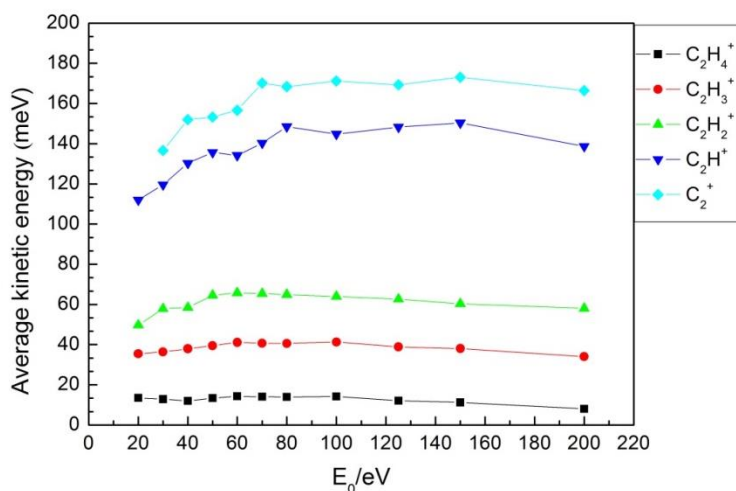


Figure 5. The average kinetic energy of different fragment ions as a function of the incident energy

The average kinetic energy for ions $C_2H_n^+$ ($n = 0-4$) has been deduced and shown in figure 5 as a function of the incident electron energy. With increasing the incident electron energy, more reaction channels with higher dissociation energies become open. Accordingly, the average kinetic energy for ions $C_2H_2^+$, C_2H^+ , C_2^+ increases at first and finally becomes saturated. For $C_2H_3^+$ ions the average kinetic energy has no dependence on the incident electron energy at least as seen in the present measurement. However, the value we obtained (~ 40 meV) is much smaller than the previous measurement [6].

The total kinetic energy release can be estimated from the average kinetic energy [6]. If the excitation of a precursor ion above the dissociation limit leads to decay into two fragments. \bar{E}_0 and \bar{E}_1 are the average kinetic energies of the precursor ion with mass m_0 and the product ion with mass m_1 respectively. Then, the total kinetic energy release \bar{E}_K is given by:

$$\bar{E}_K = \frac{\bar{E}_1 \cdot m_0}{m_0 - m_1} - \frac{\bar{E}_0 \cdot m_1}{m_0 - m_1} \quad (4)$$

For dissociation pathway (1) and (2), the KERs are 0.76 eV and 0.73 eV, respectively. The energy distribution of $C_2H_4^+$ give a direct view of the experimental energy resolution, which is an upper limit as an result of all experimental uncertainty factors including thermal energy. For the uncertainty of KER, as we deduced it from the average kinetic energy of fragment ions, with contribution of statistic uncertainty for averaging, we estimated the final uncertainty is about 15%. These values are in agreement with the previous measurement performed by N. Endstrasser et al [6] within their experimental uncertainty.

4. Conclusion

The electron impact dissociative ionization of ethylene has been studied experimentally. In this paper, we report data for the formation of $C_2H_n^+$ ($n = 0 \sim 3$) relative to that of $C_2H_4^+$ as a function of incident electron energy from 20 to 200 eV. Good agreements were achieved with previous studies. By measuring the TOF and position on the detector, the kinetic energy of the fragment ions was deduced. Taking advantages of supersonic gas-jet system, the thermal contribution for kinetic energy is dramatically reduced and the resolution of the present measurement is about 12.5 meV. For the excited state of (A^2B_{3g}), the ethylene ions can dissociate to $C_2H_3^+$ or $C_2H_2^+$. However, taking into account the different dissociation energies, the kinetic energy as well as the KER for those two ions are also different. This is indicated through the kinetic energy distributions, although these distributions

contain contributions from all excited states. The average KERs for the dissociation pathways leading to the production of $C_2H_3^+$, $C_2H_2^+$ have been estimated to be 0.76 eV and 0.73 eV, respectively.

Acknowledgements

This work was carried out as a part of an IAEA Coordinated Research Project on "Light Element Atom, Molecule and Radical Behaviour in the Divertor and Edge Plasma Regions". This work was also supported by the National Magnetic Confinement Fusion Program under grant No. 2009GB106001, the National Science Foundation of China under contract No. 10904019 and Shanghai Leading Academic Discipline Project (project No. B107).

References

- [1] Janev R K *Contemporary Phys.* 2005, *46*, 121.
- [2] Janev R K and Reiter D Collision Processes of Hydrocarbon Species in Hydrogen Plasmas: II The Ethane and Propane Families; Report Forschungszentrum Julich 2002, Jul-4005.
- [3] Janev R K and Reiter D *Physics Plasma* 2004, *11*, 780.
- [4] Tian C and Vidal C R *Chem. Phys. Lett.* 1998, *288*, 499.
- [5] Popović S, Williams S and Vušković L. *Phys. Rev. A* 2006, *73*, 022711.
- [6] Endstrasser E; Zappa F; Mauracher A; Bacher A; Feil S; Bohme D K; Scheier P; Probst M and Märk T D *Int. J. Mass Spectrom.* 2009, *280*, 65.
- [7] Wang P and Vidal C R *J. Chem. Phys.* 2002, *116*, 4023.
- [8] Ward M D; King S J and Price S D *J. Chem. Phys.* 2011, *134*, 024308.
- [9] Reiter D and Janev R K *Contrib. Plasma Phys.* 2010, *50*, 986.
- [10] Popović S, Williams S, and Vušković L *Phys. Rev. A* 2006, *73*, 022711.
- [11] Osipov T; Stener M; Belkacem A; Schöffler M; Weber Th; Schmidt L; Landers A; Prior M H; Dörner R and Cocke C L, *Phys. Rev. A* 2010, *81*, 033429.
- [12] Poll H U; Grill V; Matt S; Abramzon N; Becker K; Scheier P and Märk T D, *Int. J. Mass Spectrom.* 1998, *177*, 143.
- [13] Feil S; Gluch K; Bacher A; Matt-Leubner S; Böhme D K; Scheier P and Märk T D, *J. Chem. Phys.* 2006, *124*, 214307.
- [14] Myung H K; Brain D L; Lei S and Arther G S, *J. Chem. Phys. A* 2007, *111*, 7472.
- [15] Jiang Y H; Rudenko A; Herrwerth O; Foucar L; Kurka M; Kühnel K U; Lezius M; Kling M F; Tilborg J V; Belkacem A; Ueda K; Düsterer S; Treusch R; Schröter C D; Moshhammer R and Ullrich J, *Phys. Rev. Lett.* 2010, *105*, 263002
- [16] Gluch K, Scheier P, Schustereder W, Tempnual T, Feketeova L, Mair C, Matt-Leubner S, Stamatovic A and Märk T D *Int. J. Mass Spectrom.* 2003, *228*, 307
- [17] Lin S, Chen Z, Wei B, Wang X, Lu D, Hutton R and Zou Y, *Phys. Scr.* 2011 T144, 014095.
- [18] Wei B, Chen Z, Wang X, Lu D, Lin S, Hutton R, and Zou Y, *J. Phys. B.* 2013 *46*, 215205